

# Entangling Two Macroscopic Mechanical Resonators at High Temperature

Qing Lin<sup>1</sup>, Bing He<sup>2,\*</sup> and Min Xiao<sup>3</sup>

<sup>1</sup>*Fujian Key Laboratory of Light Propagation and Transformation, College of Information Science and Engineering, Huaqiao University, Xiamen 361021, China*

<sup>2</sup>*Center for Quantum Optics and Quantum Information, Universidad Mayor, Camino La Pirámide 5750, Huechuraba, Chile*

<sup>3</sup>*Department of Physics, University of Arkansas, Fayetteville, Arkansas 72701, USA*

 (Received 24 September 2019; revised manuscript received 12 February 2020; accepted 28 February 2020; published 11 March 2020)

At high temperature, thermal decoherence dominates so that the entanglement of quantum states is difficult to preserve. Realizing high-temperature entanglement is, therefore, a challenge to the current quantum technologies. Here, we demonstrate that considerable degrees of continuous-variable entanglement between two macroscopic objects placed in an environment of high temperature can be created through the medium of properly prepared light fields coupled to them. There are two steps to make such entanglement. First, by pumping an optical cavity field pressuring on a mechanical resonator as a macroscopic object with a blue-detuned drive field, the competition between the induced squeezing effect due to the blue-detuned drive and the existing thermal decoherence leads to a stable entanglement between the cavity field and mechanical resonator. A condition for realizing field-resonator entanglement is determined at any temperature and for any given optomechanical system. The second step is to entangle two distant mechanical resonators through a procedure of entanglement swapping. A detailed example of illustrating this entanglement swapping shows that a considerable degree of entanglement between the two mechanical resonators can be created. The current study proposes a route toward high-temperature entanglement in a realistic physical system.

DOI: [10.1103/PhysRevApplied.13.034030](https://doi.org/10.1103/PhysRevApplied.13.034030)

## I. INTRODUCTION

A majority of realistic quantum systems are open ones coupled to their environments. The influence from the environment, which is generally termed as the “reservoir,” exhibits the overall effect known as decoherence [1–3], leading to the phenomena such as entanglement sudden death (ESD) [4,5], i.e., the entanglement of a quantum system is killed by the environmental decoherence after a finite period of time. In particular, the decoherence from thermal environment is significant to quantum systems, so that most of the quantum-information processing systems should operate at ultra-low temperature [6–12], except for a few purely optical ones (see, e.g., [13–16]). Possibly preserving quantum entanglement at high temperature is especially important to practical applications as well as to fundamental researches.

A cavity optomechanical system (OMS) is a type of few-body system that is used as a platform to realize the macroscopic quantum states with various potential applications [17–19]. Entanglement of the nanomechanical resonator to the cavity field has been a phenomenon attracting

wide interest since a decade ago (see, e.g., [20–29]). But the generation of such entanglement is a nontrivial task. A reported experimental realization of optomechanical entanglement [30] follows the scenario of pulsed optomechanics [31–34]. That is to apply a red-detuned pulse first to cool the mechanical resonator down to ground state, and then entangle the mechanical resonator with another blue-detuned pulse. The obtained entanglement is verified with one more red-detuned pulse, which swaps the optomechanical entanglement to the entanglement between two pulsed fields. The whole entanglement generation and verification procedure was performed at a low temperature  $T < 20$  mK. How to overcome the low-temperature restriction and make optomechanical entanglement at higher temperature is significantly meaningful to the relevant experimental researches. Moreover, it is even more interesting to generate the entanglement between two mechanical resonators, which can be preserved for a long period of time.

In an OMS, the mechanical resonator with its frequency  $\omega_m$  and damping rate  $\gamma_m$  undergoes a significant thermal decoherence at high temperature, as the thermal decoherence rate  $R(n) = (n + 1)n_{\text{th}}\gamma_m + n(n_{\text{th}} + 1)\gamma_m$  [19,35] for a Fock-state component  $|n\rangle$  of the mechanical quantum state grows linearly with the energy level  $n$  and the thermal

\*bing.he@umayor.cl

occupation  $n_{\text{th}} = [e^{\hbar\omega_m/(k_B T)} - 1]^{-1}$  ( $\hbar$  is Planck's constant and  $k_B$  the Boltzmann constant) of the reservoir at the temperature  $T$ . To neglect the thermal decoherence over one period of mechanical oscillation, the mechanical resonator with the quality factor  $Q = \omega_m/\gamma_m$  should meet the relation  $Q\omega_m/(2\pi) > k_B T/h$  [19]. The correspondingly generalized condition,  $Q/n_{\text{th}} \gg 1$ , should be satisfied for an OMS to be unaffected from the decoherence of its thermal environment (see, e.g., [31,36,37]). Intuitively this condition should also hold for the existence of any quantum property of OMS including the entanglement between cavity field and mechanical resonator. We, however, prove below that the condition for the existence of optomechanical entanglement in thermal environment can be much more relaxed even possibly to the extent of  $Q/n_{\text{th}} < 1$ , given a suitable coupling between the cavity field and mechanical resonator. This relaxed condition makes it possible to entangle two mechanical resonators.

Besides the studies with some specific systems (see, e.g., [34,38–42]), the realization of entanglement at higher temperature has been explored with some abstract systems of coupled harmonic oscillators [43–45]. These previous studies [43–45] indicate that such entanglement should be generated with time-dependent interaction and out of thermal equilibrium with the environment. For any system, however, entanglement is created by the mutual interaction between its subsystems. If one simply makes the mutual interaction stronger (the interaction can be time independent too), will it be possible for the entanglement to survive in an environment of higher temperature? Previously there had been no quantitative results regarding this conjecture. In this work, we tackle the problem with the example of OMS, showing the possibility to offset the decoherence on entanglement with a proper coupling between cavity field and mechanical resonator.

An even more interesting problem is how to create the entanglement between two macroscopic objects located in an environment of high temperature. Though there are some experimental evidences [46,47] that quantum correlations at room temperature do exist, entanglement between two macroscopic objects at room temperature or even higher temperature has not been seen experimentally thus far. Based on the field-resonator entanglement or optomechanical entanglement mentioned above, we show that the entanglement between two mechanical resonators can be realized by a method of entanglement swapping as described in Fig. 1. If the quality factors of the two mechanical resonators are sufficiently high, such entanglement at a high temperature can be preserved for a considerable period of time.

The rest of the paper is organized as follows. In Sec. II we provide the detailed theoretical tools for calculating the optomechanical entanglement generated by blue-detuned drives, which cannot lead to time-independent steady states of an OMS. Since the field-resonator or

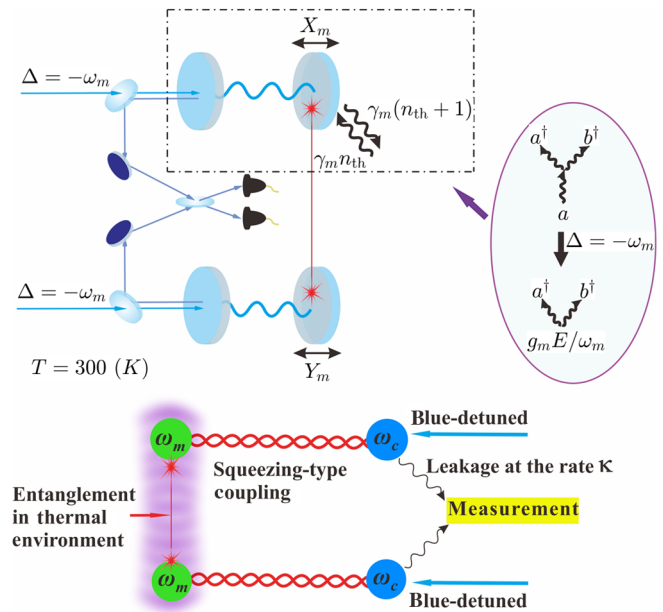


FIG. 1. Scheme for realizing the entanglement between two mechanical resonators, which independently vibrate with the displacement  $x_m$  and  $y_m$ , respectively. Here each optical cavity coupled to a mechanical resonator is driven by a strong pump field blue detuned by the frequency  $\omega_m$  of the mechanical resonator. As indicated inside the eclipse, under the blue-detuned driving field, the nonlinear optomechanical coupling due to the radiation pressure can be well approximated with a two-mode squeezing action of the intensity  $g_m E/\omega_m$ . The lower panel synthesizes the main features in the process. Each mechanical resonator is initially placed in thermal equilibrium with its environment, which can be at high temperature. The cavity fields coupled to them are driven by a blue-detuned external field, respectively, so that there is no time-independent steady state in the end (due to the induced squeezing-type coupling). By employing an entanglement swapping procedure, which is realized by measuring the leaked light out of the cavities, the two mechanical resonators are entangled.

optomechanical entanglement is the foundation for the whole scheme, we elaborate on its properties in a number of ensuing sections. In Secs. III and IV, we demonstrate various properties of optomechanical entanglement. The condition for such optomechanical or field-resonator entanglement at high temperature is illustrated in Sec. V, and the experimental feasibility is discussed in Sec. VI. Before concluding with more discussions, we demonstrate with a detailed example in Sec. VII about how the entanglement between two resonators is realized by means of entanglement swapping. In addition, there is one appendix about the non-Markovian mechanical noise.

## II. QUANTUM OPTOMECHANICAL DYNAMICS UNDER BLUE-DETUNED DRIVE

Most previous theoretical descriptions of weakly coupled quantum OMS are based on a linearization of the

system's nonlinear dynamics by a procedure described as follows (see, e.g., [20–27,31]): (1) shifting the cavity-field mode  $\hat{a} \rightarrow \hat{a} + \alpha$  with respect to its mean-field value  $\alpha(t)$  and the mechanical mode  $\hat{b} \rightarrow \hat{b} + \beta$  with respect to its average displacement  $\beta(t)$ ; (2) neglecting the resulting nonlinear terms treated as the higher-order terms of the fluctuations around the mean values  $\alpha(t)$  and  $\beta(t)$ . In the linearized Hamiltonian obtained through the procedure, the effective coupling intensity of the cavity field with the mechanical resonator becomes  $g_m|\alpha| = g_m(n_p)^{1/2}$ , where  $g_m$  is the optomechanical coupling intensity at the single-photon level and  $n_p$  the average cavity photon number. However, except for the time-independent steady-state solutions, the exact form of time-dependent mean values  $\alpha(t)$ ,  $\beta(t)$  are generally difficult to obtain. The previous treatment of pulsed drive field usually adopted certain approximations for these time-dependent averaged values [30,31]. With regard to the optomechanical entanglement due to cw drives, time-independent steady state in dynamical stability is a prerequisite to the majority of previous theoretical studies, including those about the entanglement in a higher-temperature environment, which realize dynamical stability with red-detuned drive [25] or one blue-detuned drive together with another red-detuned drive acting on an ancillary cavity [48]. Under a single blue-detuned cw drive, the steady states exist only for very weak optomechanical coupling [49], so the dynamical instability associated with blue-detuned cw drives imposes a fundamental limit on the applicability of the previous approach to quantum optomechanics [23]. As demonstrated by experiment [30], blue-detuned drive field is the main cause of optomechanical entanglement. The quantum entanglement between cavity field and mechanical resonator can surely exist, even when an OMS is not dynamically stable under a blue-detuned cw drive. In what follows we develop a method from Refs. [50–54] to deal with the quantum dynamics due to blue-detuned cw drives.

Our starting point is from the initial quantum state

$$\rho(0) = |0\rangle_c \langle 0| \otimes \sum_{n=0}^{\infty} \frac{n_{\text{th}}^n}{(1+n_{\text{th}})^{n+1}} |n\rangle_m \langle n| \quad (1)$$

of a concerned OMS, as the product of a cavity vacuum state and a mechanical thermal state before turning on the drive field. Here the mechanical reservoir with the occupation  $n_{\text{th}}$  can be at arbitrary temperature, as long as the resonator is prepared under the thermal equilibrium with its environment. An important feature of an OMS is that it is an open quantum system. The cavity and mechanical thermal reservoir of the OMS can be modeled as the ensembles of oscillators with the continuous distributions of their frequencies (the notation  $\hbar = 1$  is used in this

section):

$$H_R = \int_0^{\infty} d\omega_1 \omega_1 \hat{\xi}_c^\dagger \hat{\xi}_c(\omega_1) + \int_0^{\infty} d\omega_2 \omega_2 \hat{\xi}_m^\dagger \hat{\xi}_m(\omega_2). \quad (2)$$

The coupling of the OMS with the environment modeled by the above Hamiltonian takes the general form

$$H_{\text{SR}} = i \int d\omega_1 \kappa(\omega_1) (\hat{a} - \hat{a}^\dagger) \{ \hat{\xi}_c^\dagger(\omega_1) + \hat{\xi}_c(\omega_1) \} \\ + i \int d\omega_2 \gamma_m(\omega_2) (\hat{b} - \hat{b}^\dagger) \{ \hat{\xi}_m^\dagger(\omega_2) + \hat{\xi}_m(\omega_2) \}. \quad (3)$$

The action of the system-reservoir coupling is irreversible, giving rise to the damping of the cavity (mechanical) mode at the rate  $\kappa$  ( $\gamma_m$ ). For the smooth coupling between the system and reservoirs, the coupling intensities can be reduced to the constants, i.e.,  $\kappa(\omega) \rightarrow (\kappa/\pi)^{1/2}$ ,  $\gamma_m(\omega) \rightarrow (\gamma_m/\pi)^{1/2}$  [35].

The physical elements in the OMS include a drive from an external pump field as well as the coupling between the cavity field and mechanical resonator due to the radiation pressure. In a rotating frame with respect to the external drive frequency  $\omega_l$ , the Hamiltonians for these processes read [19]

$$H_S = \Delta \hat{a}^\dagger \hat{a} + \omega_m \hat{b}^\dagger \hat{b} + iE(\hat{a}^\dagger - \hat{a}) \quad (4)$$

and

$$H_{\text{OM}} = -g_m \hat{a}^\dagger \hat{a} (\hat{b} + \hat{b}^\dagger), \quad (5)$$

where  $\Delta = \omega_c - \omega_l$  is the detuning of the drive field's central frequency, and the driving amplitude is related to the pump power  $P$  as  $E = \sqrt{\kappa P/\omega_l}$ . The driving amplitude  $E(t)$  can be time dependent to include pulsed fields. All physical properties of a quantum OMS are the consequence of the evolution from its initial quantum state Eq. (1) under the action

$$U(t) = \mathcal{T} \exp \left\{ -i \int_0^t d\tau (H_S + H_{\text{OM}} + H_{\text{SR}} + H_R)(\tau) \right\}$$

of the total Hamiltonian including that of the stochastic part  $H_{\text{SR}}$  [35]. The quantum state  $\rho_r$  of the reservoirs is assumed to be invariant under the action, since the environment is unaffected by the concerned system.

Next we take an interaction picture with respect to the Hamiltonian  $H_S + H_R$ . The corresponding unitary transformation  $U_0(t) = \exp\{-i(H_S + H_R)t\}$  (an ordinary exponential due to the commutativity of  $H_S + H_R$  at different time)

transforms all involved operators to

$$\begin{aligned}\hat{a} &\rightarrow \hat{A}(t) = U_0^\dagger(t)\hat{a}U_0(t) = e^{-i\Delta t}[\hat{a} + D(t)], \\ \hat{b} &\rightarrow U_0^\dagger(t)\hat{b}U_0(t) = e^{-i\omega_m t}\hat{b}, \\ \hat{\xi}_c(\omega_1) &\rightarrow e^{-i\omega_1 t}\hat{\xi}_c(\omega_1), \\ \hat{\xi}_m(\omega_2) &\rightarrow e^{-i\omega_2 t}\hat{\xi}_m(\omega_2),\end{aligned}\quad (6)$$

having the displacement

$$D(t) = \int_0^t d\tau e^{i\Delta(t-\tau)} E = \frac{e^{i\Delta t} - 1}{\Delta} E \quad (7)$$

for the cavity mode. Note that, unlike a similar procedure in the routine linearization mentioned at the beginning of the section, there is no term containing the damping rate  $\kappa$  in the displacement  $D(t)$ . Then the rest of the total Hamiltonian becomes

$$\begin{aligned}H_{\text{eff}}(t) &= U_0^\dagger(t)(H_{\text{OM}} + H_{\text{SR}})U_0(t) \\ &= -g_m [D(t)\hat{a}^\dagger + D^*(t)\hat{a} + |D(t)|^2] \\ &\quad \times (e^{-i\omega_m t}\hat{b} + e^{i\omega_m t}\hat{b}^\dagger) \\ &\quad \underbrace{-g_m \hat{a}^\dagger \hat{a} (e^{-i\omega_m t}\hat{b} + e^{i\omega_m t}\hat{b}^\dagger)}_{H_N(t)}\end{aligned}$$

$$\begin{aligned}\langle \hat{O}(t) \rangle &= \text{Tr}_S\{\hat{O}\rho(t)\} = \text{Tr}_S\{\hat{O}\text{Tr}_R[U(t)\rho(0)\rho_r U^\dagger(t)]\} \\ &= \text{Tr}_{S,R}\{\hat{O}U_0(t)\mathcal{T}e^{-i\int_0^t d\tau H_{\text{eff}}(\tau)}\rho(0)\rho_r\mathcal{T}e^{i\int_0^t d\tau H_{\text{eff}}(\tau)}U_0^\dagger(t)\} \\ &= \text{Tr}_{S,R}\{\mathcal{T}e^{i\int_0^t d\tau U_N(t,\tau)(H_{\text{eff}}-H_N)(\tau)}U_N^\dagger(t,\tau)U_0^\dagger(t)\hat{O}U_0(t)\mathcal{T}e^{-i\int_0^t d\tau U_N(t,\tau)(H_{\text{eff}}-H_N)(\tau)}U_N^\dagger(t,\tau)U_N(t,0)\rho(0)\rho_r U_N^\dagger(t,0)\} \\ &\approx \text{Tr}_{S,R}\{\mathcal{T}e^{i\int_0^t d\tau (H_{\text{eff}}-H_N)(\tau)}U_0^\dagger(t)\hat{O}U_0(t)\mathcal{T}e^{-i\int_0^t d\tau (H_{\text{eff}}-H_N)(\tau)}\rho(0)\rho_r\},\end{aligned}\quad (10)$$

in which the trace is taken over both the system part  $S$  and the reservoir part  $R$ . As emphasized in Ref. [35], the action  $U(t)$  in the above is only a formally unitary one, since it also involves the action of the system-reservoir couplings that cause the damping of the system modes as the nonunitary processes. The interaction picture with  $U_0(t)$  as mentioned above is equivalent to the factorization of the operator  $U(t)$  on the second line of Eq. (10). To determine the effect of the nonlinear term  $H_N(t)$  in Eq. (8), we continue to factorize its action  $U_N(t,0) = \mathcal{T} \exp\{-i\int_0^t dt' H_N(t')\}$  out of the evolution operator  $\mathcal{T} \exp\{-i\int_0^t d\tau H_{\text{eff}}(\tau)\}$  as in Eq. (10). The operation  $U_N(t,0)$  factorized out in Eq. (10) keeps the initial quantum state  $\rho(0)\rho_r$  invariant since the cavity is initially in a vacuum state  $|0\rangle_c$ . In both

$$\begin{aligned}&+ i\sqrt{2\kappa}\{e^{-i\Delta t}\hat{A}^\dagger(t)\hat{\xi}_c(t) - e^{i\Delta t}\hat{A}(t)\hat{\xi}_c^\dagger(t)\} \\ &+ i\sqrt{2\gamma_m}[\hat{b}^\dagger\hat{\xi}_m(t) - \hat{b}\hat{\xi}_m^\dagger(t)],\end{aligned}\quad (8)$$

where

$$\begin{aligned}\hat{\xi}_c(t) &= \frac{1}{\sqrt{2\pi}} \int d\omega \hat{\xi}_c(\omega) e^{-i(\omega-\Delta)t}, \\ \hat{\xi}_m(t) &= \frac{1}{\sqrt{2\pi}} \int d\omega \hat{\xi}_m(\omega) e^{-i(\omega-\omega_m)t}.\end{aligned}\quad (9)$$

In the above Eq. (8) we apply the rotating-wave approximation to neglect the terms containing the fast oscillating factors in the system-reservoir coupling part. Like almost all other researches in quantum optomechanics (see, e.g., the review articles [19,55]), we treat the noise operators in Eq. (9) as the white ones with the correlations  $\langle \hat{\xi}_c(t)\hat{\xi}_c^\dagger(t') \rangle = \delta(t-t')$  and  $\langle \hat{\xi}_m(t)\hat{\xi}_m^\dagger(t') \rangle_R = (n_{\text{th}} + 1)\delta(t-t')$ , where  $n_{\text{th}}$  is the thermal occupation. The discussion on the more realistic non-Markovian thermal noise is given in the Appendix.

The essential point in our approach is a proper use of the effective Hamiltonian, Eq. (8), for finding the expectation values of the evolved system operators (including those as the observables in experiments). The expectation value of an arbitrary operator  $\hat{O}(t) = U^\dagger(t)\hat{O}U(t)$  that evolves with time can be written as

of the factorization procedures, we only perform the truly unitary operations to modify the system mode operators in the remaining Hamiltonians, to avoid the actually nonunitary action by the system-reservoir coupling  $H_{\text{SR}}$  used in Ref. [50]. The transformed operators  $U_N(t,\tau)\hat{a}U_N^\dagger(t,\tau)$  and  $U_N(t,\tau)\hat{b}U_N^\dagger(t,\tau)$  in Eq. (10) differ from the original ones,  $\hat{a}$  and  $\hat{b}$ , by the terms in the orders of  $g_m/\omega_m$ , and such corrections can be neglected for a weakly coupled OMS satisfying  $g_m/\omega_m \ll 1$  (especially in the highly resolved sideband regime  $\omega_m/\kappa \gg 1$ ). Throughout our derivations, the approximation sign in Eq. (10) due to this practice is the only step that is not exact, in addition to the commonly used Markovian approximation [19,55] and rotation-wave approximation for the noise terms.

Finding the value of  $\langle \hat{O}(t) \rangle$  can be, therefore, reduced to determining the evolved operator  $\hat{O}(t)$  due to the successive actions  $U_0(t)$  and  $\mathcal{T} \exp\{-i \int_0^t d\tau (H_{\text{eff}} - H_N)(\tau)\}$ , and then taking its expectation value with respect to the fixed initial quantum state  $\rho(0)\rho_r$ . The evolved operator  $\hat{O}(t)$  may contain the quantum-noise operators, whose averages over the total reservoir state  $\rho_r$  should be found by the correlation relations of the noise operators in Eq. (9). The first action  $U_0(t)$  evolves the system operators exactly as in Eq. (6). The evolutions of the operators  $\hat{O} = \hat{a}$  and  $\hat{b}$  under the second action  $\mathcal{T} \exp\{-i \int_0^t d\tau (H_{\text{eff}} - H_N)(\tau)\}$  of a quadratic Hamiltonian are determined by the corresponding dynamical equations that are in the exact forms as well. Making use of the proper Ito rules for the quantum-noise operators in the system-reservoir coupling part [35], one obtains the dynamical equations as follows:

$$\begin{aligned} \dot{\hat{a}} &= -\kappa \hat{a} + i g_m D(t) (e^{-i\omega_m t} \hat{b} + e^{i\omega_m t} \hat{b}^\dagger) - \kappa D(t) \\ &\quad + \sqrt{2\kappa} \hat{\xi}_c(t), \\ \dot{\hat{b}} &= -\gamma_m \hat{b} + i g_m e^{i\omega_m t} [D(t) \hat{a}^\dagger + D^*(t) \hat{a}] \\ &\quad + i g_m e^{i\omega_m t} |D(t)|^2 + \sqrt{2\gamma_m} \hat{\xi}_m(t). \end{aligned} \quad (11)$$

These linear differential equations including the coherent and noise drive terms can be numerically tackled. As seen from the equations, the effect of the coupling terms of squeezing type, which are proportional to  $\hat{a}^\dagger$  or  $\hat{b}^\dagger$  on their right sides, can be significantly enhanced by a blue-detuned cw drive set at  $\Delta = -\omega_m$ . After plugging in the displacement  $D(t)$  [see Eq. (7)] with  $\Delta = -\omega_m$ , there are such coupling terms without oscillating phase factor, which are equivalent to a resonant two-mode squeezing Hamiltonian

$$H_{\text{coupling}} = J(\hat{a}\hat{b} + \hat{a}^\dagger\hat{b}^\dagger), \quad (12)$$

where  $J = g_m E / \omega_m$ ; this coupling dominates in the process illustrated in the lower panel of Fig. 1, and contributes significantly to optomechanical entanglement. The squeezing effect manifests more explicitly from the corresponding equations

$$\begin{aligned} \dot{\hat{a}} &= -\kappa \hat{a} + J \hat{b}^\dagger + i \kappa g_m^{-1} J + \sqrt{2\kappa} \hat{\xi}_c(t), \\ \dot{\hat{b}} &= -\gamma_m \hat{b} + J \hat{a}^\dagger - i g_m^{-1} J^2 + \sqrt{2\gamma_m} \hat{\xi}_m(t) \end{aligned} \quad (13)$$

in the limit  $\omega_m / \kappa \rightarrow \infty$ , since the effects of the other coupling terms carrying oscillating factors are completely averaged out in this limit. It is impossible to stop the mechanical resonator in a squeezing-dominant situation, and its final motion is a steady oscillation after introducing the nonlinear saturation.

The quantum states of an OMS evolved from the initial state  $\rho(0)$  in Eq. (1) are Gaussian states, if the evolution

process can be approximated with the successive actions of  $U_0(t)$  and  $\mathcal{T} \exp\{-i \int_0^t d\tau (H_{\text{eff}} - H_N)(\tau)\}$  as in Eq. (10). The information about such Gaussian states is contained in the  $4 \times 4$  correlation matrix (CM)

$$\hat{V} = \begin{pmatrix} \hat{A} & \hat{C} \\ \hat{C}^T & \hat{B} \end{pmatrix}, \quad (14)$$

with its elements defined as

$$V_{ij}(t) = \frac{1}{2} \langle \delta \hat{u}_i(t) \delta \hat{u}_j(t) + \delta \hat{u}_j(t) \delta \hat{u}_i(t) \rangle. \quad (15)$$

Here the fluctuation  $\delta \hat{u}_i(t) = \hat{u}_i(t) - \langle \hat{u}_i(t) \rangle$  is around the time-dependent expectation value  $\langle \hat{u}_i(t) \rangle$  for the elements of the vector  $\hat{u}(t) = [\hat{X}_c(t), \hat{P}_c(t), \hat{X}_m(t), \hat{P}_m(t)]^T$ , where  $\hat{X}_l = (\hat{c} + \hat{c}^\dagger)/2^{1/2}$ ,  $\hat{P}_l = -i(\hat{c} - \hat{c}^\dagger)/2^{1/2}$  for  $l = c, m$  and  $c = a, b$ . In contrast, in the majority of the previous studies confined to the regimes of red-detuned cw drive or weak blue-detuned cw drive, the expectation values  $\langle \hat{u}_i(t) \rangle$  should be time-independent steady ones. Our concerned time-dependent CM elements for the quantum states of any weakly coupled OMS can be found from Eqs. (10) and (11), directly giving the Wigner functions of its evolving Gaussian states. A measure for the corresponding entanglement between the cavity and mechanical modes is the logarithmic negativity  $E_{\mathcal{N}} = \max[0, -\ln(2\eta^-)]$  [56–59], where

$$\eta^- = \sqrt{\Sigma - \sqrt{\Sigma^2 - 4 \det \hat{V}} / \sqrt{2}} \quad (16)$$

and  $\Sigma = \det \hat{A} + \det \hat{B} - 2 \det \hat{C}$ . So far we develop the theoretical tools that deals with the optomechanical entanglement due to blue-detuned cw drives.

### III. OPTOMECHANICAL ENTANGLEMENT DUE TO BLUE-DETTUNED DRIVE

In this section we present the detailed results of the evolved optomechanical entanglement due to a cw pump laser set at the squeezing resonant point  $\Delta = -\omega_m$ . The effects of the noise drive terms in this situation are intensified as well, so one expects significant decoherence from the cavity and mechanical reservoir, which could totally eliminate the quantum features. On the other hand, a significantly enhanced two-mode squeezing effect at  $\Delta = -\omega_m$  is beneficial to entangling the cavity field and mechanical resonator. The realized entanglement is obviously the result of the competition between these two factors. In addition to the entanglement, we consider the purity of the

evolved state  $\rho(t)$  [60]

$$\mu[\rho(t)] = \text{Tr}\rho^2(t) = \frac{1}{4\sqrt{\text{Det}\hat{V}(t)}}, \quad (17)$$

where  $\hat{V}$  is the CM defined in Eq. (14), as a figure-of-merit for the two-mode system's resistance against thermal decoherence. The evolution tendency of the entanglement is compared with the corresponding tendency of the purity.

For an OMS at room temperature we first look at its associate cavity photon number  $\langle \hat{a}^\dagger(t)\hat{a}(t) \rangle = |\alpha(t)|^2$ . This average cavity photon number evolves according to the following nonlinear dynamical equations:

$$\begin{aligned} \dot{\alpha} &= -\kappa\alpha + ig_m(e^{-i\omega_m t}\beta + \beta^*e^{i\omega_m t})\alpha + Ee^{i\Delta t}, \\ \dot{\beta} &= -\gamma_m\beta + ig_m|\alpha|^2 \end{aligned} \quad (18)$$

in the frame rotating at the resonant cavity frequency  $\omega_c$  and the mechanical frequency  $\omega_m$ , where  $\alpha = \langle \hat{a} \rangle$  and  $\beta = \langle \hat{b} \rangle$ . As shown in Fig. 2(a), due to the two-mode squeezing effect under the blue-detuned drive, the cavity photon number increases quickly at the beginning evolution period and then stabilizes under the nonlinear saturation. To calculate the quantum coherence and entanglement, however, the system dynamics should be linearized. In its initial thermal state, the mechanical resonator's fluctuation magnitude  $\langle \delta\hat{b}^\dagger\delta\hat{b} \rangle$  has been far above the corresponding mean value  $|\beta(0)|^2 = 0$  already, so it is impossible to adopt the routine linearization approach mentioned at the beginning of Sec. II.

Figures 2(b) and 2(c) show the evolved quantum purity and quantum entanglement according to our linearized dynamics detailed in Sec. II. According to Eq. (11), which

is valid at the beginning evolution period for the system of nonlinear dynamics, these quantities stabilize after a period of time before the system enters the nonlinear regime, i.e., the time scales for the stabilization of  $\mu$  and  $E_{\mathcal{N}}$  are much shorter than the time for the cavity photon number to stabilize. It is a consequence of the balance of the total decoherence and effective optomechanical coupling. The significant decoherence that exists in the processes manifests by the completely vanishing purities in Fig. 2(b), though their initial values are rather low at room temperature. Under the dominant squeezing effect, the determinant of the CM in Eq. (17) diverges, inevitably eliminating the remnant purity of any initially prepared state. On the other hand, the entanglement magnitude is determined by the factor  $\Sigma(t) - [\Sigma^2(t) - 4\det\hat{V}(t)]^{1/2}$  in Eq. (16). With the progress of an evolution, the subtraction of the two diverging terms in the factor converges to a stably oscillating function, resulting in the illustrated entanglement.

An interesting phenomenon with the higher drive intensity is the significantly oscillating magnitude of the entanglement. The cause for such oscillation is relevant to the oscillating coupling terms in Eq. (11). One can see the point by increasing the sideband resolution  $\omega_m/\kappa$ . In the limit  $\omega_m/\kappa \rightarrow \infty$ , the oscillating terms in the dynamical equations takes no effect, to reduce the dynamical equations to Eq. (13). The stable entanglement value in this limit has an analytical form

$$E_{\mathcal{N}} = -\ln \left[ \frac{J^2(\kappa + 2\gamma_m n_{\text{th}}) - (\kappa\sqrt{4J^2 + \kappa^2} - \kappa^2)\gamma_m n_{\text{th}}}{J^2\sqrt{4J^2 + \kappa^2}} \right] \quad (19)$$

under the realizable condition  $\kappa \gg \gamma_m$ . As shown in Fig. 3, the oscillating entanglement values numerically

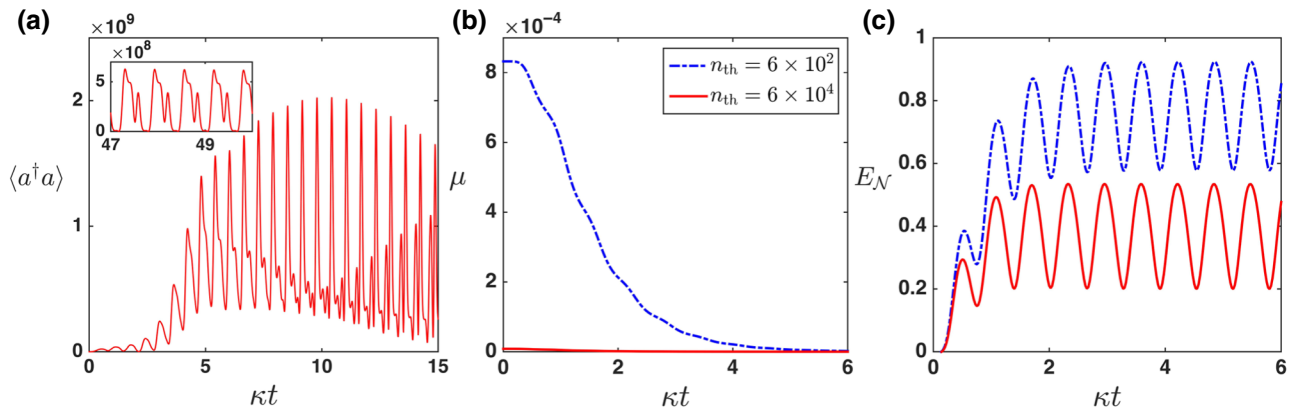


FIG. 2. Real-time evolutions of cavity photon number, purity, and entanglement in thermal environment. In (a) we consider the room temperature  $T = 300$  K for a mechanical resonator with the frequency  $\omega_m/2\pi = 100$  MHz, and the system is driven by a blue-detuned ( $\Delta/\omega_m = -1$ ) cw pump field with the amplitude  $E/\kappa = 10^5$ . The inset in (a) shows the stabilized cavity photon number evolved according to the nonlinear dynamical equations, in contrast to the growing cavity photon in the linear dynamical regime. In (b) and (c), two initial temperatures corresponding to the indicated different thermal occupations are used for the evolutions of the purity and entanglement. The parameters for the system are taken as  $g_m/\kappa = 10^{-4}$ ,  $\omega_m/\kappa = 10$ , and  $Q = \omega_m/\gamma_m = 10^6$ .

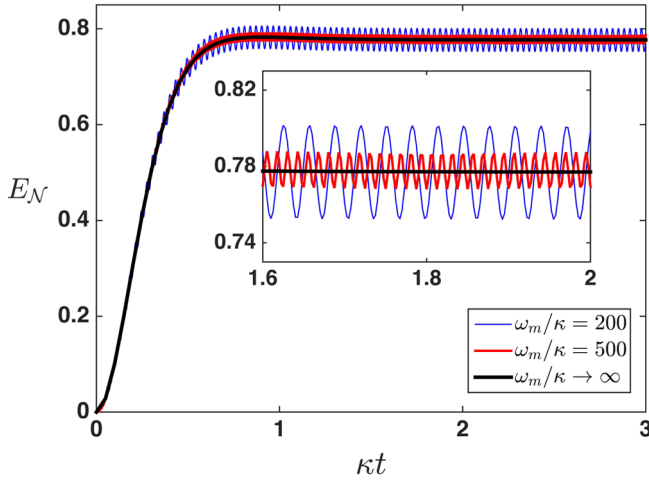


FIG. 3. Evolved entanglement for the setups with  $\omega_m/\kappa \gg 1$ . The system parameters are  $g_m/\kappa = 10^{-4}$ ,  $Q = 10^6$ . The drive intensity and the thermal reservoir occupation are set to satisfy the relations  $J/\kappa = (g_m/\omega_m)(E/\kappa) = 2.5$  and  $(\gamma_m/\kappa)n_{\text{th}} = 1$ .

calculated according to Eq. (11) asymptotically tends to this steady result. This completely steady entanglement obtained from Eq. (13) with only constant coupling terms distinguishes our scenario from the previous proposals of high-temperature entanglement [43–45], where time-dependent interaction is indispensable.

#### IV. HOW OPTOMECHANICAL ENTANGLEMENT STABILIZES

From the above discussions one sees that optomechanical entanglement under blue-detuned cw drive can exist at sufficiently high temperature. The technically achievable OMSs with their mechanical quality factors  $Q = 10^5 - 10^6$  [19] are good candidates for the purpose, as the decoherence, especially the thermal one at high temperature, can be overcome by a proper mutual interaction. We also see from the illustrated examples that the decoherence effect on entanglement is totally different from the corresponding effect on the coherence as the loss of purity. The causes for such uniqueness in the generated entanglement should be identified.

We find out what determines the entanglement dynamics from the dynamical equations, Eq. (11). In the equations, the decoherence from the cavity and mechanical reservoirs acts as the quantum-noise terms proportional to  $(2\kappa)^{1/2}$  and  $(2\gamma_m)^{1/2}$ , respectively. If removing these terms, the associated entanglement evolves according to a dynamics without the decoherence from environment. Under the enhanced two-mode squeezing due to a blue-detuned cw drive field, the optomechanical entanglement grows monotonously with time under such assumed dynamics; see the pink curves in Fig. 4. To see the effects of the different types of quantum noise, one can separately add

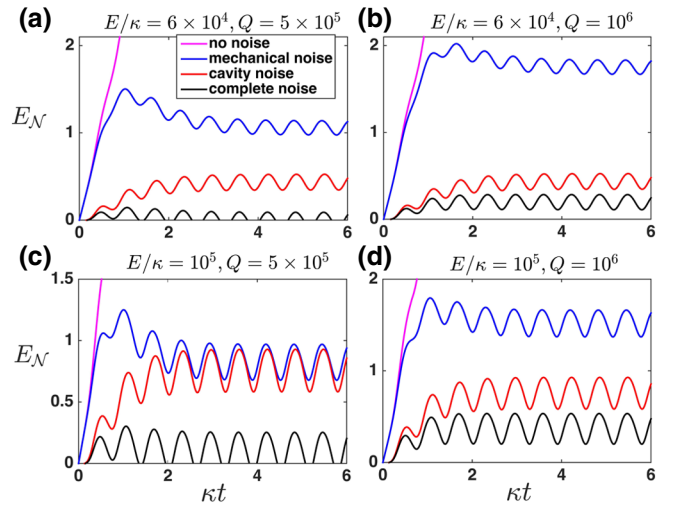


FIG. 4. Comparison of the entanglement values with and without quantum-noise effects. Here we calculate the logarithmic negativity for the entanglement evolved with only the cavity noise, with only the mechanical noise and under both the cavity and mechanical noises, respectively. The other system parameters, which are not indicated here, are the same as those in Fig. 2.

the noise drive terms back to the equations. Only with the mechanical noise term  $(2\gamma_m)^{1/2}\hat{\xi}_m$  in Eq. (11), the evolved entanglement becomes stabilized oscillation. A larger quality factor  $Q$  is found to suppress the thermal noise effect, by comparing the blue curves in Figs. 4(a) and 4(c) with the corresponding ones in Figs. 4(b) and 4(d). As compared with the mechanical noise, the effect of the cavity noise, which obviously leads to the lower values of stabilized entanglement, is more significant in these examples. The existence of any type of noise can obviously affect the concerned entanglement, in contrast to the simple modification of cavity photon numbers and other quantities by the noises [61–63].

The larger oscillation amplitude for a realized entanglement under the stronger drive exists to the entanglement stabilized under any type of the noises. From the examples in Fig. 4, one sees that a stronger noise effect actually displaces the entanglement values under fix drive intensity  $E$  to the lower side along the vertical axis. With the combined effect from both the cavity and mechanical noises, the realized optomechanical entanglement as its stabilized value shifted towards the horizontal axis, can exhibit periodic ESD and entanglement revival; see the black curves in Figs. 4(a) and 4(c). For clearer illustrations of the balanced decoherence and optomechanical coupling, which affect the evolution of our concerned entanglement, we apply the further increased drive power to one of the setups considered in Fig. 4. The results of their evolutions are given in Fig. 5. Except for the obvious change at the beginning steps of raising the drive intensity (the two figures on the

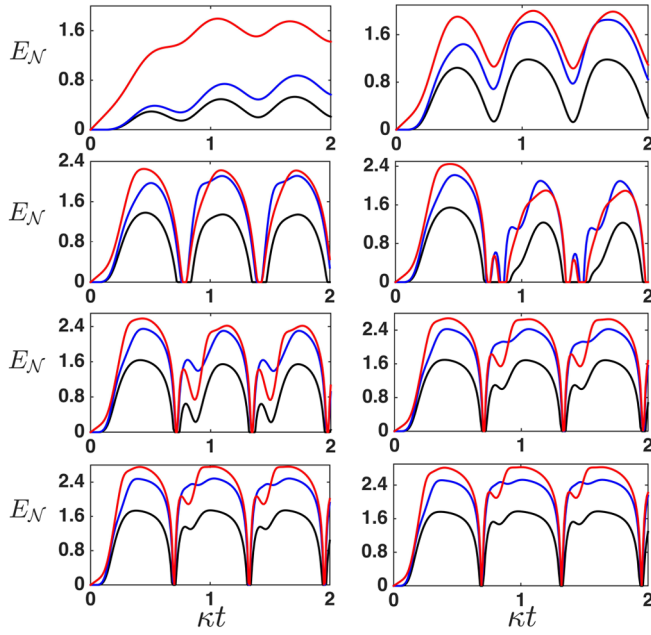


FIG. 5. Evolved entanglement with a series of gradually increased drive intensity. Following the order from the upper left frame to the lower right frame, the drive intensity  $E/\kappa$  grows from  $10^5$  to  $2.4 \times 10^6$  with a gap of  $2 \times 10^5$  for each step. The system parameters are the same as those in Fig. 4 with a fixed  $Q = 10^6$ . The colors of the curves are in one-to-one correspondence with those in Fig. 4.

first row of Fig. 5), the evolution of the entanglement varies little in spite of adding more drive power successively. The effects of creating and killing the entanglement, both of which become more significant with increased drive power, can well balance each other over a considerable range of the drive intensity.

### V. CONDITION FOR REALIZING HIGH-TEMPERATURE OPTOMECHANICAL ENTANGLEMENT

The most interesting issue for our concerned optomechanical entanglement is how it could survive at high temperature. For a simple quantum mechanical oscillator under thermal decoherence, which has the number of coherent oscillations as  $\omega_m/(\gamma_m n_{\text{th}}) = Q f_m [h/(k_B T)]$  [ $f_m = \omega_m/(2\pi)$ ], its decoupling from the thermal environment's influence should satisfy the condition  $Q/n_{\text{th}} \gg 1$ , where  $n_{\text{th}} = k_B T/(\hbar \omega_m)$  for the oscillator at high temperature. Under this condition the purity of the quantum states of an OMS may be preserved, as mentioned in the previous studies (see, e.g., [36,37]). To the quantum entanglement of the OMS, however, an extra factor is the coupling between the cavity and mechanical modes as the mutual interaction to create the entanglement. As understand from the above discussions, the stabilized entanglement due to blue-detuned cw drive is the result of the balanced decoherence and

mutual interaction, both of which become larger with time in the concerned regime of dynamical instability. Could such a balance be reset by a proper optomechanical coupling so that the entanglement can appear with the lower ratio  $Q/n_{\text{th}}$  for the systems?

This conjecture can be solved by finding the direct relation of the evolved entanglement with the ratio  $Q/n_{\text{th}}$ . Considering the possible appearance of ESD and entanglement revival as in Figs. 4(a) and 4(c), we here use the stable peak value of the entanglement to indicate its existence. The setup in Fig. 2 is used to illustrate the entanglement in general thermal environment, with a flexibility that its mechanical quality factor can be adjusted in preparing the setup. The results in Fig. 6(a) show that the optomechanical entanglement can appear with a proper drive intensity as long as the concerned ratio is in the order  $Q/n_{\text{th}} \sim 1$ , which is much more relaxed than the condition  $Q/n_{\text{th}} \gg 1$  for an OMS to be decoupled from

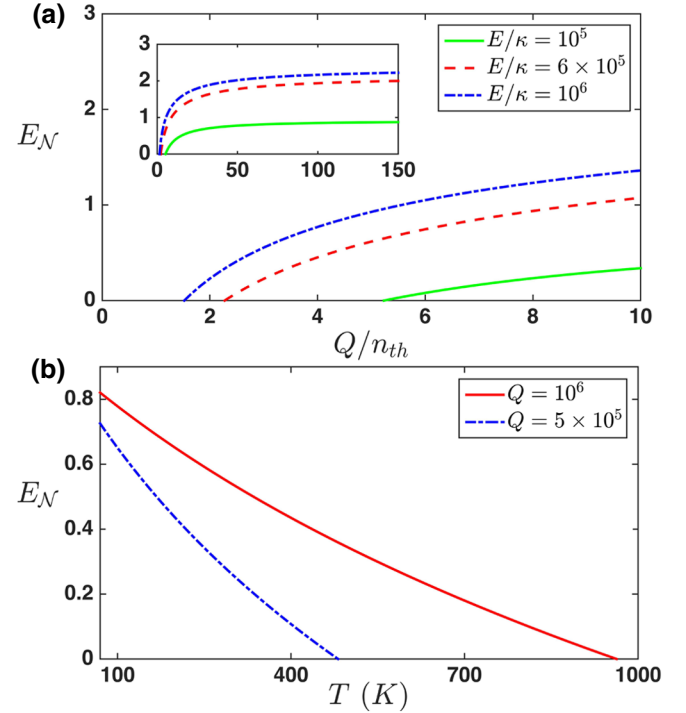


FIG. 6. Relations between the achieved peak value entanglement with the temperature and mechanical quality factor. (a) The ratio  $Q/n_{\text{th}}$  for the existence of optomechanical entanglement. For all the given drive intensities, the entanglement appears with the ratio in the order of  $Q/n_{\text{th}} \sim 1$ . The inset shows a saturation of the values of the stabilized entanglement. With the even higher drive intensities, the entanglement may exist at a point  $Q/n_{\text{th}} < 1$ . (b) The tendency of the stabilized peak values of entanglement, which are obtained given the drive intensity  $E/\kappa = 10^5$ , with the temperature up to the degree higher than 900 K for a technically available quality factor  $Q = 10^6$ . In both (a) and (b) we have  $\omega_m/2\pi = 100$  MHz, and  $g_m/\kappa = 10^{-4}$ ,  $\omega_m/\kappa = 10$ ,  $\Delta/\omega_m = -1$  as in Fig. 2.

thermal decoherence. The modified balance between decoherence and optomechanical coupling due to the change of system parameters in the evolution of entanglement can be seen in Fig. 6(a). For instance, at the fixed point  $Q/n_{\text{th}} = 2$ , no entanglement exists under the drives of lower intensity ( $E/\kappa = 10^5, 6 \times 10^5$ ), but a higher intensity ( $E/\kappa = 10^6$ ) inducing a more significant coupling than the simultaneously intensified decoherence can give rise to a nonzero entanglement up to the order of  $E_{\mathcal{N}} = 0.1$ . As seen from the inset of Fig. 6(a), a very high ratio  $Q/n_{\text{th}}$  cannot improve on the entanglement forever because of the decoherence from the cavity reservoir, which takes an independent action on the system. In terms of the temperature of the thermal reservoir, one can illustrate the general tendency of the entanglement as in Fig. 6(b). It is possible to have entanglement at much higher than room temperature, given the technically achievable quality factor  $Q$  as those in Fig. 6(b). Unlike the previous proposals (see, e.g., [20–26]), such robust entanglement should be realized in the regime without time-independent steady state.

A further question is how to estimate the necessary interaction (optomechanical coupling) for the realization of the entanglement at a certain temperature. The reciprocal of the ratio  $Q/n_{\text{th}}$  is proportional to the factor  $(\gamma_m/\kappa)n_{\text{th}}$ , which indicates the thermal decoherence rate from the mechanical reservoir. The realized entanglement is the result of the system dynamical evolution determined by the effective optomechanical couplings as well as by the decoherence from the reservoirs. An intuitive model for understanding the main features of the system dynamics is the one in the limit  $\omega_m/\kappa \rightarrow \infty$ , whose dynamical equations are Eq. (13). After rewriting the dynamical equations in terms of the dimensionless time scale  $\kappa t$ , one sees that all evolved quantities according to the equations change only with three parameters  $J/\kappa$ ,  $\gamma_m/\kappa$ , and  $n_{\text{th}}$ . Under the condition  $\gamma_m/\kappa \ll 1$ , the finally stable entanglement can also be given as an analytical form in Eq. (19). The stable entanglement distribution in this limit [see Fig. 7(b)] is like a deformation of the corresponding distribution for a finite sideband resolution  $\omega_m/\kappa = 10$  in Fig. 7(a). A difference for the finite sideband resolution, however, is that boundary for the existence of entanglement slowly crosses the position  $Q/n_{\text{th}} = 1$  with the increasing effective coupling  $J/\kappa$  [see Fig. 7(a)]. As an example, the system with  $g_m/\kappa = 10^{-4}$  and driven by a blue-detuned cw drive with  $E/\kappa = 10^7$  can have an averaged stable entanglement of  $E_{\mathcal{N}} \approx 0.093$ , when the mechanical resonator having  $\omega_m/\kappa = 10$  and  $\gamma_m/\kappa = 1/900$  is in a thermal environment with  $n_{\text{th}} = 10^4$ . The ratio  $Q/n_{\text{th}}$  in this case is only 0.9.

In the limit  $\omega_m/\kappa \rightarrow \infty$  considered in Fig. 7(b), there is a clear boundary on the left of the diagonal line ( $\gamma_m n_{\text{th}} = g_m E/\omega_m$ ) in this figure for the existence of entanglement. For a fixed thermal decoherence at the rate  $(\gamma_m/\kappa)n_{\text{th}}$ ,

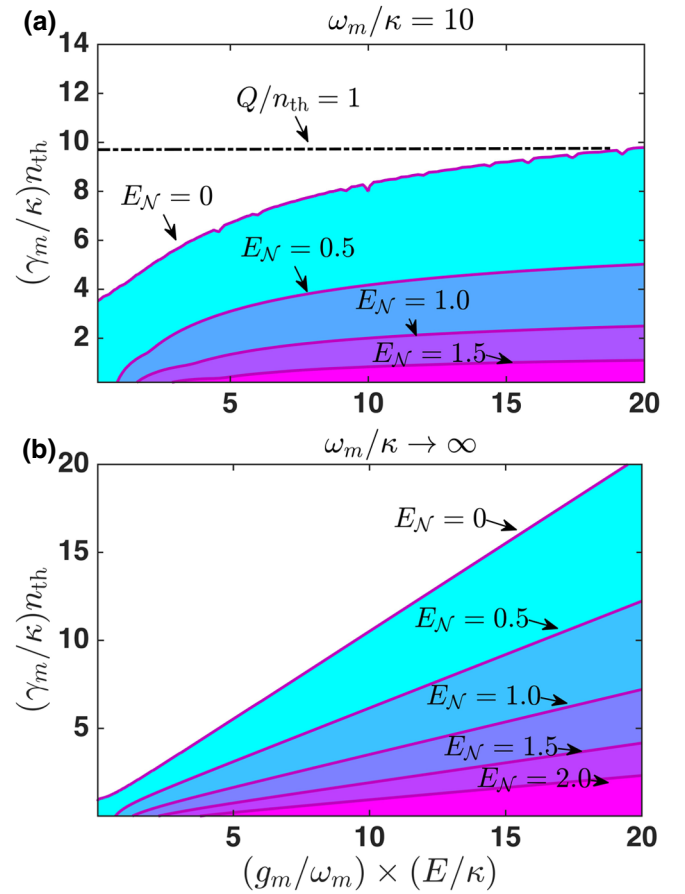


FIG. 7. (a) Stabilized value of entanglement with Eq. (11) in the space of the parameters  $J/\kappa = g_m E/(\omega_m \kappa)$  and  $(\gamma_m/\kappa)n_{\text{th}}$ , with  $g_m/\kappa = 10^{-4}$ ,  $\omega_m/\kappa = 10$ ,  $Q = 10^6$ . The optomechanical coupling intensity on the general level is indicated by the first parameter, and the general thermal decoherence rate is measured by the second parameter. (b) The analytical entanglement with Eq. (19) in the space of the same parameters as in (a).

the following condition

$$J = g_m E/\omega_m \geq \gamma_m n_{\text{th}} \quad (20)$$

is sufficient to obtain the optomechanical entanglement with a certain drive power that realizes the proper coupling intensity. Due to the possible adjustment of the effective coupling intensity  $J$ , optomechanical entanglement satisfying the condition can be realized even with a ratio  $Q/n_{\text{th}} < 1$ . The OMSs with  $\omega_m/\kappa \gg 1$ , which are relevant to the relation, are experimentally realized thus far (see, e.g., [64]).

## VI. EXPERIMENTAL FEASIBILITY

According to the criterion provided in the above discussions, the two quantities ( $J = g_m E/\omega_m$  and  $Q = \omega_m/\gamma_m$ )

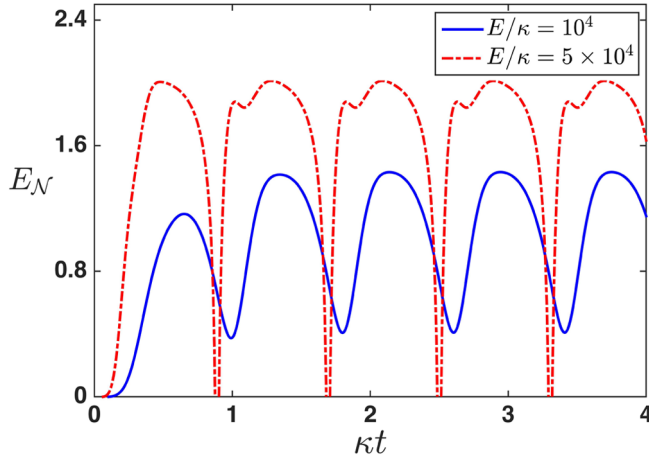


FIG. 8. Entanglement that can be achieved with the experimental setup in Ref. [65], which operates at optical frequency and has the parameters  $\omega_m/2\pi = 3 \times 10^9$  Hz,  $\kappa/2\pi = 5 \times 10^8$  Hz,  $g_m/2\pi = 9 \times 10^5$  Hz, and  $Q = 10^5$ . Here we consider its performance at the room temperature  $T = 300$  K corresponding to  $n_{\text{th}} = 1.6 \times 10^3$ .

that a setup can have are crucial to experimental generation of optomechanical entanglement at a certain temperature  $T$ . If they can properly operate under the intensified cavity field due to blue-detuned drives, almost all previously reported systems generates more or less such optomechanical entanglement simply by changing the frequencies of the drives. Better systems can also be designed according to the criterion for generating the demanded optomechanical entanglement.

Without loss of generality, we consider one of the previously reported experimental setups, which was used to perform an experiment of cooling mechanical resonator to ground state [65]. But the setup is operated at the room temperature now. In Fig. 8, we demonstrate its evolved entanglement by respectively applying two drives of different intensities. The magnitudes of the realized stable entanglement are seen to be sufficiently high. Under the stronger drive amplitude the average degree of entanglement is even higher, since it brings about a stronger squeezing effect. The entanglement realized by the weaker drive (the solid blue curve in Fig. 8) requires a pumping laser with the power of approximate 40 mW. Other systems with high  $Q$ , such as those in Refs. [64,66], are also possible for the implementation.

## VII. ENTANGLING TWO MECHANICAL RESONATORS THROUGH ENTANGLEMENT SWAPPING

After we obtain a stabilized optomechanical entanglement, it is possible to connect it with another optomechanical entanglement to make the entanglement between

two mechanical resonators. This procedure of entanglement swapping is described in Figs. 1 and 9. After the two optomechanical entanglements are stabilized, their two CMs completely contain the information about these two independently generated entanglements. To describe the entanglement swapping process, we start from the Wigner function of the total system, which takes the form

$$W(X_1, X_2) = \mathcal{N} \exp \left\{ -\frac{1}{2} X_1^T \hat{V}_1^{-1} X_1 - \frac{1}{2} X_2^T \hat{V}_2^{-1} X_2 \right\}, \quad (21)$$

where  $\mathcal{N}$  is a normalization coefficient, and  $X_1 = (X_c^1, P_c^1, X_m^1, P_m^1)^T$ ,  $X_2 = (X_c^2, P_c^2, X_m^2, P_m^2)^T$  are the vectors of dynamical variables. The output fields from the cavities are related to their inputs and the cavity modes  $\hat{a}^i$  as [67]

$$\hat{a}_{\text{out}}^i(t) = \sqrt{\kappa} \hat{a}^i - \hat{a}_{\text{in}}^i(t), \quad (22)$$

for  $i = 1, 2$ . Because the input and output fields propagate toward two opposite directions, the ones leaking out of the cavities and to be measured are  $\sqrt{\kappa} \hat{a}^1$  and  $\sqrt{\kappa} \hat{a}^2$ , respectively (we assume an equal damping rate  $\kappa$  for the two cavities).

First, we let these fields from the cavities interfere with one another through a 50:50 beam splitter (BS) as in Fig. 9(a), to have the following transformations:

$$\begin{aligned} X_c^{1'} &= (\sqrt{\kappa} X_c^1 + \sqrt{\kappa} X_c^2) / \sqrt{2}, \\ X_c^{2'} &= (\sqrt{\kappa} X_c^1 - \sqrt{\kappa} X_c^2) / \sqrt{2}, \\ P_c^{1'} &= (\sqrt{\kappa} P_c^1 + \sqrt{\kappa} P_c^2) / \sqrt{2}, \\ P_c^{2'} &= (\sqrt{\kappa} P_c^1 - \sqrt{\kappa} P_c^2) / \sqrt{2}. \end{aligned} \quad (23)$$

In the Wigner function of the system, the variables  $X_c^1$ ,  $X_c^2$  and  $P_c^1$ ,  $P_c^2$  are to be replaced by the linear combinations of  $X_c^{1'}/\sqrt{\kappa}$ ,  $X_c^{2'}/\sqrt{\kappa}$ ,  $P_c^{1'}/\sqrt{\kappa}$ , and  $P_c^{2'}/\sqrt{\kappa}$ , as

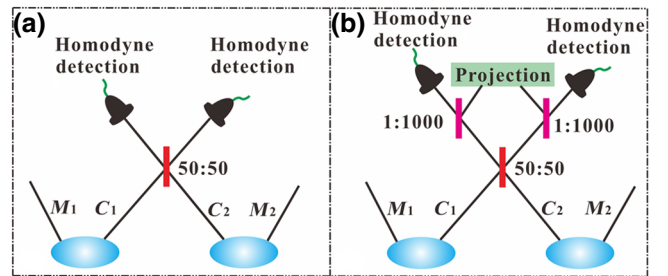


FIG. 9. Entanglement swapping. (a) The output two cavity modes ( $C_1$  and  $C_2$  as the intrinsic cavity modes multiplied by  $\sqrt{\kappa}$ ) interfere through a 50:50 beam splitter (BS) and two of the output modes are measured. (b) The two output modes after the first 50:50 BS are transmitted into two 1:1000 BS, respectively. The weak modes are measured while the strong modes are projected out.

the inverse transformation of the above. Then we measure the modes  $X_c^{1'}$  and  $P_c^{2'}$ , and have the results  $X_c^{1'}/\sqrt{\kappa}$  and  $P_c^{2'}/\sqrt{\kappa}$  to be substituted into the Wigner function. The resulting Wigner function of the two mechanical resonators should be obtained by integrating out the two other variables  $P_c^{1'}/\sqrt{\kappa}$  and  $X_c^{2'}/\sqrt{\kappa}$ , because they cannot be measured simultaneously due to the uncertainty relation for the noncommuting operators. The Wigner function  $W(X_m^1, X_m^2)$  obtained in this way exactly describes the quantum state and the associated entanglement. The corresponding CM and the associated logarithmic negativity indicate the mechanical entanglement after the swapping procedure is performed.

The above entanglement swapping can be implemented in principle, but the measurement of cavity modes through a homodyne detection [68–70] is difficult for the strong intensities of the output cavity modes, which exists under blue-detuning drives. To implement the swapping procedure more conveniently, one can add two more BSs in addition to the two output modes of the 50:50 BS as shown in Fig. 9(b). The reflectivity of the two extra BSs can be high, e.g., 99.9% or even higher. In other words, we separate one output cavity mode to one weak and one strong field, respectively. The strong one is projected out, while the weak one is to be measured through a homodyne detection. The desired entanglement swapping can still be achieved with a suitable detection system that is available thus far.

Now we use an experimentally achievable system used in Fig. 8 for an example of such entanglement swapping. The environment temperature here is set to be  $T = 300$  K. We select two slightly different time points for the two subsystems of optomechanics (the equality of the moments for the measurement of them can also be taken if assuming an ideal set), and get the two entangled states of the two independent optomechanical systems. The corresponding logarithmic negativities are  $E_{\mathcal{N}}^1 = 1.310$  and  $E_{\mathcal{N}}^2 = 1.271$ , respectively. Following the processes presented above, the finally obtained quantum state of the two mechanical resonators has a logarithmic negativity  $E_{\mathcal{N}}^m = 0.396$ , which is the degree of entanglement between the two mechanical resonators after the entanglement swapping is implemented.

## VIII. DISCUSSION AND CONCLUSION

Quantum entanglement has two prominent features. One is its ubiquitousness due to interaction [71], and the other is its fragility under decoherence [4,5]. By intuition, thermal decoherence at high temperature may kill any type of entanglement. Finding the proper balance between decoherence and interaction to make entanglement in thermal environment is meaningful to potential applications.

Our current work proposes a method for realizing quantum entanglement of two macroscopic objects at room temperature or even higher temperatures.

Recently, the existence of quantum correlations at room temperature has been experimentally investigated [46,47]. The quantum fluctuations considered in these experiments are around the steady states of a system. In the current work we present a method to deal with the associated fluctuations around time-dependent cavity field and mechanical displacement of weakly coupled OMSs, so that more flexibility could be available in more general situations. Optomechanical entanglement is a phenomenon attracting wide attention concerning the macroscopic quantum states of OMS. The uniqueness in the current study is about the creation of such entanglement with blue-detuned cw drive field, which leads to more significant two-mode squeezing effect than the red-detuned drives or blue-detuned pulses considered in the previous studies. Our analysis shows that optomechanical entanglement due to blue-detuned cw drive can become stable in thermal environment, indicating the possibility of realizing the entanglement even at very high temperature. The condition for obtaining the entanglement of OMS is found to be much more relaxed than the well-known criterion for preserving an OMS's coherence in thermal environment. Directly applying blue-detuned cw drives also simplifies the generation of optomechanical entanglement.

More technical concerns can arise in the implementation of our proposal. One of them is the continually increasing displacement of the mechanical resonator in the dynamical unstable regime due to blue-detuned drive. After the displacement proportional to the real part of  $\langle \hat{b}(t) \rangle$  is beyond an extent so that the effective dynamics of the system begins to be purely nonlinear, the mechanical motion stabilizes in a self-induced oscillation [19]. The entanglement between the cavity field and mechanical resonator, however, still exists after reaching the nonlinear regime, as it can stabilize independently before the system enters the nonlinear regime. In the current study we work with the Markovian approximation for the mechanical reservoir at high temperature. The more realistic non-Markovian noise can modify the concerned entanglement (see Appendix).

A more fundamental aspect of the current study is to understand how quantum entanglement can survive in thermal environment. The illustrated examples with OMSs demonstrate that, at high temperature, the behaviors of the coherence and entanglement are totally different. The loss of the latter due to environmental decoherence can be offset by the interaction within a system. In other words, entanglement with an object can be easier to exist than the Schrödinger cat (quantum superposition) made out of the same object. As a result, there are richer phenomena beyond the general scenario of ESD that is previously envisioned. Together with the numerical simulations in different situations, a quantitative relation Eq. (20) found

in the highly resolved sideband regime indicates how large the interaction should be required for preserving an optomechanical entanglement at any temperature. This relation about mutual interaction and thermal decoherence allows one to speculate that high-temperature entanglement can also exist in other dynamical systems.

### ACKNOWLEDGMENTS

This work is supported by Fondo de Iniciación, Universidad Mayor (código PEP I-2019021), National Natural Science Foundation of China (NSFC) (No. 11574093).

### APPENDIX: NON-MARKOVIAN THERMAL RESERVOIR

In real situations the thermal noise acting on the mechanical resonator is not exactly Markovian, so it is necessary to have a more detailed look at how the realistic non-Markovian noise can be reduced to a Markovian one at higher temperature. While some other literature adopt the Schrödinger approach (see, e.g., [72,73]), we here apply the Heisenberg-Langevin approach with the notations close to those in Ref. [35]. The mechanical noise discussed below refers to the term  $\hat{\zeta}_m(t)$  in the dynamical equation

$$\begin{aligned}\dot{\hat{X}}_m &= \omega_m \hat{P}_m, \\ \dot{\hat{P}}_m &= \underbrace{-\omega_m \hat{X}_m + g_m \hat{a}^\dagger \hat{a}}_{-V'(\hat{X}_m)} - \frac{\gamma_m}{\omega_m} \dot{\hat{X}}_m + \hat{\zeta}_m(t)\end{aligned}\quad (\text{A1})$$

of the mechanical resonator, and it is related to the mechanical noise operator in Eqs. (11) and (13) as  $\hat{\zeta}_m(t) \sim \hat{\xi}_m(t) + \hat{\xi}_m^\dagger(t)$ .

We start from the model of the thermal reservoir, which is an ensemble of oscillators coupled to the mechanical resonator. The effective Hamiltonian of the reservoir coupled to the mechanical resonator has the form [35]

$$H_{\text{th}} = \frac{1}{2} \sum_n \{(\hat{p}_n - \kappa_n \hat{X}_m)^2 + \omega_n^2 \hat{q}_n^2\}, \quad (\text{A2})$$

where  $p_n$  and  $q_n$  are the momentum and displacement of an oscillator with the frequency  $\omega_n$ . Those reservoir oscillation modes are quantum so that they satisfy  $[\hat{q}_n, \hat{p}_{n'}] = i\hbar \delta_{nn'}$  and  $[\hat{q}_n(\hat{p}_n), \hat{X}_m(\hat{P}_m)] = 0$ . From the dynamical equations

$$\begin{aligned}\dot{\hat{q}}_n &= \frac{i}{\hbar} [H_{\text{th}}, \hat{q}_n] = \hat{p}_n - \kappa_n \hat{X}_m, \\ \dot{\hat{p}}_n &= \frac{i}{\hbar} [H_{\text{th}}, \hat{p}_n] = -\omega_n^2 \hat{q}_n\end{aligned}\quad (\text{A3})$$

for the reservoir operators, one has the evolved mode

$$\begin{aligned}\hat{a}_n(t) &= e^{-i\omega_n(t-t_0)} \hat{a}_n(t_0) \\ &\quad - \kappa_n \sqrt{\frac{\omega_n}{2\hbar}} \int_{t_0}^t d\tau e^{-i\omega_n(t-\tau)} \hat{X}_m(\tau)\end{aligned}\quad (\text{A4})$$

for their linear combination  $\hat{a}_n = (\omega_n \hat{q}_n + i\hat{p}_n)/\sqrt{2\hbar\omega_n}$ . Using this evolving reservoir mode together with the effective Hamiltonian  $H_{\text{th}}$ , one obtains the dynamical equations for  $\hat{X}_m$  and  $\hat{P}_m$ :

$$\begin{aligned}\dot{\hat{X}}_m &= \omega_m \hat{P}_m, \\ \dot{\hat{P}}_m &= -V'[\hat{X}_m(t)] - \int_{t_0}^t d\tau \gamma(t-\tau) \dot{\hat{X}}_m(\tau) \\ &\quad - \gamma(t-t_0) \hat{X}_m(t_0) + \hat{\zeta}_m(t)\end{aligned}\quad (\text{A5})$$

in which there are the memory function or damping kernel

$$\gamma(t-t') = \sum_n \kappa_n^2 \cos[\omega_n(t-t')] \quad (\text{A6})$$

and, more importantly, the thermal noise operator

$$\begin{aligned}\hat{\zeta}_m(t) &= i \sum_n \kappa_n \sqrt{\frac{\omega_n}{2}} \\ &\quad \times [\hat{a}_n^\dagger(t_0) e^{i\omega_n(t-t_0)} - \hat{a}_n(t_0) e^{-i\omega_n(t-t_0)}]\end{aligned}\quad (\text{A7})$$

in terms of the reservoir modes.

The next step is to generalize the model of discrete oscillation modes in Eq. (A2) to a continuum one, which is similar to those in Eqs. (2) and (3). The memory function then becomes

$$\begin{aligned}\gamma(t-t') &= \sum_n \kappa_n^2 \cos[\omega_n(t-t')] \\ &\rightarrow \int_0^\infty \cos[\omega(t-t')] J(\omega) \frac{dn(\omega)}{d\omega} d\omega,\end{aligned}\quad (\text{A8})$$

where  $J(\omega)$  is a continuum distribution of the coupling, and  $n(\omega)$  the occupation of the modes at the frequency  $\omega$ . The derived dynamical equations, Eq. (A5), from the reservoir model reduces to the actual ones in Eq. (A1) only after imposing the relation

$$J(\omega) \frac{dn(\omega)}{d\omega} = \frac{2\gamma_m}{\pi\omega_m} \quad (\text{A9})$$

on the continuum noise spectrum, so that the memory function reduces to

$$\begin{aligned}\gamma(t-t') &= \int_0^\infty \frac{2\gamma_m}{\pi\omega_m} \cos[\omega(t-t')] d\omega \\ &= \frac{2\gamma_m}{\omega_m} \delta(t-t').\end{aligned}\quad (\text{A10})$$

In Eq. (A5) the integral  $\int_0^t d\tau \delta(t-\tau) f(\tau) = \frac{1}{2} f(t)$  is applied to have the equations reduced to Eq. (A1).

With the thermal noise operator in Eq. (A7) one can directly find the expectation value of the commutator with respect to the reservoir state  $\rho_r$ :

$$\begin{aligned} \langle [\hat{\xi}_m(t), \hat{\xi}_m(t')] \rangle_R &= i \frac{d}{dt} \gamma(t-t') \\ &= -i \frac{2\gamma_m}{\pi\omega_m} \int_0^\infty \omega \sin[\omega(t-t')] d\omega \\ &\equiv \Delta(t-t'), \end{aligned} \quad (\text{A11})$$

as well as that of the anticommutator:

$$\begin{aligned} \langle \{\hat{\xi}_m(t)\hat{\xi}_m(t') + \hat{\xi}_m(t')\hat{\xi}_m(t)\} \rangle_R &= 2 \int_0^\infty \omega J(\omega) \frac{dn}{d\omega} \left[ N(\omega) + \frac{1}{2} \right] \cos[\omega(t-t')] d\omega \\ &= \frac{2\gamma_m}{\pi\omega_m} \int_0^\infty \omega \coth\left(\frac{\hbar\omega}{2k_B T}\right) \cos[\omega(t-t')] d\omega \\ &\equiv \Delta_1(t-t'), \end{aligned} \quad (\text{A12})$$

where

$$N(\omega_n) = \langle \hat{a}_n^\dagger \hat{a}_n \rangle_R = \frac{1}{\exp\left(\frac{\hbar\omega_n}{k_B T}\right) - 1}.$$

Here we extend from the discrete to the continuum model and impose the requirement on the continuum spectrum as in Eq. (A9). These two correlations can be combined to have

$$\begin{aligned} \langle \hat{\xi}_m(t)\hat{\xi}_m(t') \rangle_R &= \frac{1}{2} [\Delta_1(t-t') + \Delta(t-t')] \\ &= \frac{\gamma_m}{\omega_m} \int_{-\infty}^\infty \frac{d\omega}{2\pi} e^{-i\omega(t-t')} \omega \\ &\quad \times \left[ \coth\left(\frac{\hbar\omega}{2k_B T}\right) + 1 \right]. \end{aligned} \quad (\text{A13})$$

In the high-temperature limit one has  $2k_B T \gg \hbar\omega$  for all relevant frequency  $\omega$  in the noise spectrum (at  $T = 10$  K, for example,  $k_B T/h \sim 10^{11}$  Hz), and then there is the approximation

$$\begin{aligned} \frac{1}{2} \langle \{\hat{\xi}_m(t)\hat{\xi}_m(t') + \hat{\xi}_m(t')\hat{\xi}_m(t)\} \rangle_R &\approx \frac{2\gamma_m k_B T}{\hbar\omega_m} \frac{1}{\pi} \int_0^\infty d\omega \cos[\omega(t-t')] \\ &= \frac{2\gamma_m k_B T}{\hbar\omega_m} \delta(t-t') \end{aligned} \quad (\text{A14})$$

for the thermal noise [see, e.g., [23] or Eq. (3.463) in Ref. [72]].

Beyond the above approximation, one can directly demonstrate how the correlation function approaches to the one like a delta function in the high-temperature limit. Because the function  $\Delta_1(t-t')$  in Eq. (A12) diverges at  $t=t'$ , we introduce a convergence factor  $\lambda$  to rewrite  $\Delta_1(t-t')$  as [35]

$$\begin{aligned} \langle \{\hat{\xi}_m(t)\hat{\xi}_m(t') + \hat{\xi}_m(t')\hat{\xi}_m(t)\} \rangle_R &= \frac{2\gamma_m}{\pi\omega_m} \int_0^\infty \left[ \omega \coth\left(\frac{\hbar\omega}{2k_B T}\right) - \omega \right] \cos[\omega(t-t')] d\omega \\ &\quad + \frac{\gamma_m}{\pi\omega_m} \int_{-\infty}^\infty |\omega| e^{i\omega(t-t')} e^{-\lambda\omega} d\omega \\ &= \frac{2\gamma_m}{\pi\omega_m} \left\{ -\left(\frac{\pi k_B T}{\hbar}\right)^2 \text{cosech}^2\left[\frac{\pi k_B T}{\hbar}(t-t')\right] \right. \\ &\quad \left. + \frac{1}{(t-t')^2} \right\} + \frac{2\gamma_m}{\pi\omega_m} \frac{\lambda^2 - (t-t')^2}{[\lambda^2 - (t-t')^2]^2}. \end{aligned} \quad (\text{A15})$$

The two pieces proportional to the constant  $2\gamma_m/(\pi\omega_m)$  converge at  $t=t'$ , respectively. When  $\lambda \rightarrow 0$ , the above correlation is

$$\begin{aligned} \langle \{\hat{\xi}_m(t)\hat{\xi}_m(t') + \hat{\xi}_m(t')\hat{\xi}_m(t)\} \rangle_R &= -\frac{2\gamma_m}{\pi\omega_m} \left(\frac{\pi k_B T}{\hbar}\right)^2 \text{cosech}^2\left[\frac{\pi k_B T}{\hbar}(t-t')\right] \\ &\approx -\frac{8\pi\gamma_m(k_B T)^2}{\hbar^2\omega_m} \exp\left\{-\frac{2\pi k_B T}{\hbar}|t-t'|\right\} \end{aligned} \quad (\text{A16})$$

as  $|t-t'| \rightarrow \infty$ . Then there naturally arises a thermal correlation time  $\hbar/(2\pi k_B T)$ . By choosing the convergence factor  $\lambda$  to be this thermal correlation time, we plot the correlation function in Eq. (A15) for some different environmental temperatures in Fig. 10. It shows that, as the

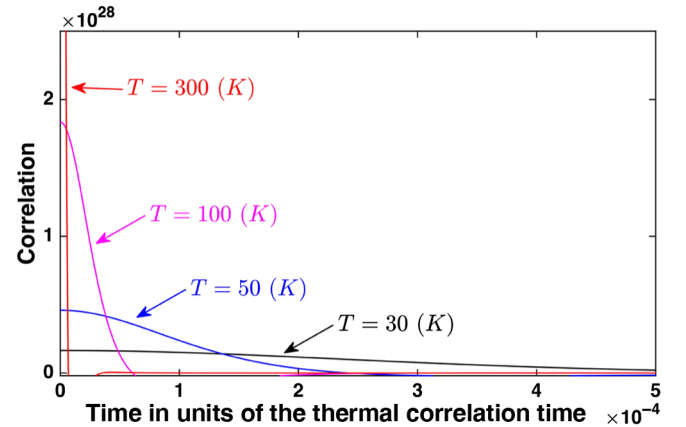


FIG. 10. Correlation functions of the thermal noise at different temperatures. The functions are calculated with the form in Eq. (A15) divided by the factor  $2\gamma_m/(\pi\omega_m)$ . The convergence factor is chosen as  $\lambda = \hbar/(2\pi k_B T)$ .

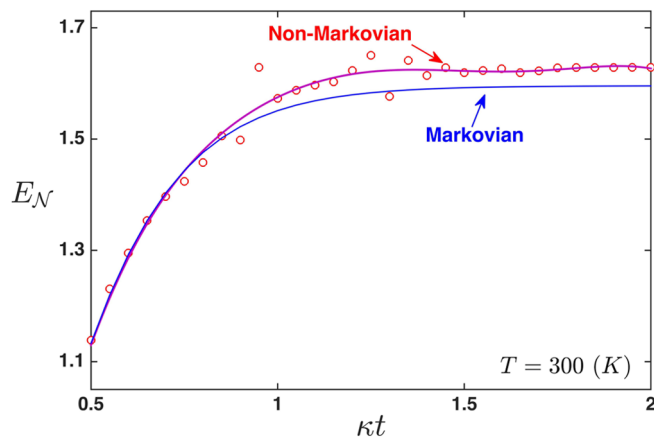


FIG. 11. Comparison of the optomechanical entanglement evolutions under the colored (non-Markovian) and the white (Markovian) mechanical noises, which are calculated in the limit  $\omega_m/\kappa \rightarrow \infty$ . The evolutions take place at room temperature, and the system parameters are chosen to be  $g_m E/\omega_m = 2.5\kappa$  and  $\gamma_m = 5 \times 10^{-4}\kappa$ .

temperature goes up, the peak value of the correlation function at  $t = t'$  grows up tremendously, and it also drops to zero quickly at a tiny nonzero  $|t - t'|$ . This provides an evidence for the validity of the white-noise approximation (with the delta-function correlation) at high temperature.

In Fig. 11 we also provide an example for comparing the evolutions of optomechanical entanglement under a colored mechanical noise with the non-Markovian correlation (A13) and the corresponding white mechanical noise with the Markovian correlation (A14). The system is operated in the highly resolved sideband limit to have a clean squeezing-type coupling between the cavity field and the mechanical resonator. The numerical simulation based on the correlation in Eq. (A13) shows no big difference of the evolution under the colored noise from the one influenced by the approximated white noise. Moreover, to the generation of entanglement, the non-Markovian or colored noise is seen to be a bit less harmful. It could be explained with its lower power, because the corresponding white noise distributes independently of the frequency and thus exerts equal force at each frequency.

[1] W. H. Zurek, Decoherence, einselection, and the quantum origins of the classical, *Rev. Mod. Phys.* **75**, 715 (2003).  
 [2] A. J. Leggett and A. Garg, Quantum Mechanics versus Macroscopic Realism: Is the Flux There When Nobody Looks? *Phys. Rev. Lett.* **54**, 857 (1985).  
 [3] A. J. Leggett, Testing the limits of quantum mechanics: Motivation, state of play, prospects, *J. Phys.: Condens. Matter* **14**, R415 (2002).  
 [4] T. Yu and J. H. Eberly, Finite-Time Disentanglement Via Spontaneous Emission, *Phys. Rev. Lett.* **93**, 140404 (2004).

[5] T. Yu and J. H. Eberly, Sudden death of entanglement, *Science* **323**, 598 (2009).  
 [6] K. Hammerer, A. S. Sørensen, and E. S. Polzik, Quantum interface between light and atomic ensembles, *Rev. Mod. Phys.* **82**, 1041 (2010).  
 [7] J. I. Cirac and P. Zoller, Quantum Computations with Cold Trapped Ions, *Phys. Rev. Lett.* **74**, 4091 (1995).  
 [8] D. Leibfried, R. Blatt, C. Monroe, and D. Wineland, Quantum dynamics of single trapped ions, *Rev. Mod. Phys.* **75**, 281 (2003).  
 [9] L.-M. Duan and C. Monroe, Colloquium: Quantum networks with trapped ions, *Rev. Mod. Phys.* **82**, 1209 (2010).  
 [10] D. Loss and D. P. DiVincenzo, Quantum computation with quantum dots, *Phys. Rev. A* **57**, 120 (1998).  
 [11] J. Q. You and F. Nori, Superconducting circuits and quantum information, *Phys. Today* **58**, 42 (2005).  
 [12] M. H. Devoret and R. J. Schoelkopf, Superconducting circuits for quantum information: An outlook, *Science* **339**, 1169 (2013).  
 [13] P. Kok, W. J. Munro, K. Nemoto, T. C. Ralph, J. P. Dowling, and G. J. Milburn, Linear optical quantum computing, *Rev. Mod. Phys.* **79**, 135 (2007).  
 [14] B. He and J. A. Bergou, A general approach to physical realization of unambiguous quantum-state discrimination, *Phys. Lett. A* **356**, 306 (2006).  
 [15] J. A. Bergou, Discrimination of quantum states, *J. Mod. Opt.* **57**, 160 (2010).  
 [16] Q. Lin and B. He, Highly efficient processing of multiphoton states, *Sci. Rep.* **5**, 12792 (2015).  
 [17] T. J. Kippenberg and K. J. Vahala, Cavity optomechanics: Back-action at the mesoscale, *Science* **321**, 1172 (2008).  
 [18] P. Meystre, A short walk through quantum optomechanics, *Ann. Phys. (Berlin)* **525**, 215 (2013).  
 [19] M. Aspelmeyer, T. J. Kippenberg, and F. Marquardt, Cavity optomechanics, *Rev. Mod. Phys.* **86**, 1391 (2014).  
 [20] D. Vitali, S. Gigan, A. Ferreira, H. R. Böhm, P. Tombesi, A. Guerreiro, V. Vedral, A. Zeilinger, and M. Aspelmeyer, Optomechanical Entanglement between a Movable Mirror and a Cavity Field, *Phys. Rev. Lett.* **98**, 030405 (2007).  
 [21] M. Paternostro, D. Vitali, S. Gigan, M. S. Kim, C. Brukner, J. Eisert, and M. Aspelmeyer, Creating and Probing Multipartite Macroscopic Entanglement with Light, *Phys. Rev. Lett.* **99**, 250401 (2007).  
 [22] D. Vitali, P. Tombesi, M. J. Woolley, A. C. Doherty, and G. J. Milburn, Entangling a nanomechanical resonator and a superconducting microwave cavity, *Phys. Rev. A* **76**, 042336 (2007).  
 [23] C. Genes, A. Mari, P. Tombesi, and D. Vitali, Robust entanglement of a micromechanical resonator with output optical fields, *Phys. Rev. A* **78**, 032316 (2008).  
 [24] M. J. Hartmann and M. B. Plenio, Steady State Entanglement in the Mechanical Vibrations of Two Dielectric Membranes, *Phys. Rev. Lett.* **101**, 200503 (2008).  
 [25] C.-L. Zou, X.-B. Zou, F.-W. Sun, Z.-F. Han, and G.-C. Guo, Room-temperature steady-state optomechanical entanglement on a chip, *Phys. Rev. A* **84**, 032317 (2011).  
 [26] M. Abdi, S. Barzanjeh, P. Tombesi, and D. Vitali, Effect of phase noise on the generation of stationary entanglement in cavity optomechanics, *Phys. Rev. A* **84**, 032325 (2011).

- [27] Q. Lin, B. He, R. Ghobadi, and C. Simon, Fully quantum approach to optomechanical entanglement, *Phys. Rev. A* **90**, 022309 (2014).
- [28] Q. Lin and B. He, Optomechanical entanglement under pulse drive, *Opt. Express* **23**, 24497 (2015).
- [29] Z.-X. Chen, Q. Lin, B. He, and Z.-Y. Lin, Entanglement dynamics in double-cavity optomechanical systems, *Opt. Express* **25**, 17237 (2017).
- [30] T. A. Palomaki, J. D. Teufel, R. W. Simmonds, and K. W. Lehnert, Entangling mechanical motion with microwave fields, *Science* **342**, 710 (2013).
- [31] S. G. Hofer, W. Wieczorek, M. Aspelmeyer, and K. Hammerer, Quantum entanglement and teleportation in pulsed cavity optomechanics, *Phys. Rev. A* **84**, 052327 (2011).
- [32] M. R. Vanner, I. Pikovski, G. D. Cole, M. S. Kim, C. Brukner, K. Hammerer, G. J. Milburn, and M. Aspelmeyer, Pulsed quantum optomechanics, *Proc. Natl. Acad. Sci. U.S.A.* **108**, 16182 (2011).
- [33] M. R. Vanner, J. Hofer, G. D. Cole, and M. Aspelmeyer, Cooling-by-measurement and mechanical state tomography via pulsed optomechanics, *Nat. Commun.* **4**, 2295 (2013).
- [34] A. A. Rakhubovsky and R. Filip, Robust entanglement with a thermal mechanical oscillator, *Phys. Rev. A* **91**, 062317 (2015).
- [35] C. W. Gardiner and P. Zoller, *Quantum Noise* (Springer Verlag, Berlin Heidelberg, 2000).
- [36] W. Marshall, C. Simon, R. Penrose, and D. Bouwmeester, Towards Quantum Superpositions of a Mirror, *Phys. Rev. Lett.* **91**, 130401 (2003).
- [37] U. Akram, W. P. Bowen, and G. J. Milburn, Entangled mechanical cat states via conditional single photon optomechanics, *New J. Phys.* **15**, 093007 (2013).
- [38] V. Vedral, High-temperature macroscopic entanglement, *New J. Phys.* **6**, 102 (2004).
- [39] F. Benatti, R. Floreanini, and U. Marzolino, Environment induced entanglement in a refined weak-coupling limit, *Europhys. Lett.* **88**, 20011 (2009).
- [40] F. Benatti, R. Floreanini, and U. Marzolino, Entangling two unequal atoms through a common bath, *Phys. Rev. A* **81**, 012105 (2010).
- [41] D. Florian, I. Jakobi, B. Naydenov, N. Zhao, S. Pezzagna, C. Trautmann, J. Meijer, P. Neumann, F. Jelezko, and Jörg Wrachtrup, Room-temperature entanglement between single defect spins in diamond, *Nat. Phys.* **9**, 139 (2013).
- [42] P. V. Klimov, A. L. Falk, D. J. Christle, V. V. Dobrovitski, and D. D. Awschalom, Quantum entanglement at ambient conditions in a macroscopic solid-state spin ensemble, *Sci. Adv.* **1**, e1501015 (2015).
- [43] F. Galve, L. A. Pachón, and D. Zueco, Bringing Entanglement to the High Temperature Limit, *Phys. Rev. Lett.* **105**, 180501 (2010).
- [44] J.-T. Hsiang and B. L. Hu, Quantum entanglement at high temperatures? Bosonic systems in nonequilibrium steady state, *J. High Energy Phys.* **11**, 090 (2015).
- [45] A. F. Estrada and L. A. Pachon, Quantum limit for driven linear non-markovian open-quantum-Systems, *New J. Phys.* **17**, 033038 (2015).
- [46] T. P. Purdy, K. E. Grutter, K. Srinivasan, and J. M. Taylor, Quantum correlations from a room-temperature optomechanical cavity, *Science* **356**, 1265 (2017).
- [47] V. Sudhir, R. Schilling, S. A. Fedorov, H. Schütz, D. J. Wilson, and T. J. Kippenberg, Quantum Correlations of Light from a Room Temperature Mechanical Oscillator for Force Metrology, *Phys. Rev. X* **7**, 031055 (2017).
- [48] T. Wang, L. Wang, Y.-M. Liu, C.-H. Bai, D.-Y. Wang, H.-F. Wang, and S. Zhang, Temperature-resistant generation of robust entanglement with blue-detuning driving and mechanical gain, *Opt. Express* **27**, 29581 (2019).
- [49] M. Ludwig, B. Kubala, and F. Marquardt, The optomechanical instability in the quantum regime, *New J. Phys.* **10**, 095013 (2008).
- [50] B. He, Quantum optomechanics beyond linearization, *Phys. Rev. A* **85**, 063820 (2012).
- [51] B. He, L. Yang, and M. Xiao, Dynamical phonon laser in coupled active-passive microresonators, *Phys. Rev. A* **94**, 031802(R) (2016).
- [52] B. He, L. Yang, Q. Lin, and M. Xiao, Radiation Pressure Cooling as a Quantum Dynamical Process, *Phys. Rev. Lett.* **118**, 233604 (2017).
- [53] Q. Lin and B. He, Highly efficient cooling of mechanical resonator with square pulse drives, *Opt. Express* **26**, 33830 (2018).
- [54] C. Wang, Q. Lin, and B. He, Breaking the optomechanical cooling limit by two drive fields on a membrane-in-the-middle system, *Phys. Rev. A* **99**, 023829 (2019).
- [55] C. Genes, A. Mari, D. Vitali, and P. Tombesi, Quantum effects in optomechanical systems, *Adv. At. Mol. Opt. Phys.* **57**, 33 (2009).
- [56] G. Vidal and R. F. Werner, Computable measure of entanglement, *Phys. Rev. A* **65**, 032314 (2002).
- [57] G. Adesso, A. Serafini, and F. Illuminati, Extremal entanglement and mixedness in continuous variable systems, *Phys. Rev. A* **70**, 022318 (2004).
- [58] M. B. Plenio, The Logarithmic Negativity: A Full Entanglement Monotone That is not Convex, *Phys. Rev. Lett.* **95**, 090503 (2005).
- [59] C. Weedbrook, S. Pirandola, R. Garcia-Patron, N. J. Cerf, T. C. Ralph, J. H. Shapiro, and S. Lloyd, Gaussian quantum information, *Rev. Mod. Phys.* **84**, 621 (2012).
- [60] S. Olivares, Quantum optics in the phase space – A tutorial on Gaussian states, *Eur. Phys. J. Spec. Top.* **203**, 3 (2012).
- [61] G. S. Agarwal and K. Qu, Spontaneous generation of photons in transmission of quantum fields in PT-symmetric optical systems, *Phys. Rev. A* **85**, 031802(R) (2012).
- [62] B. He, L. Yang, Z. Zhang, and M. Xiao, Cyclic permutation-time symmetric structure with coupled gain-loss microcavities, *Phys. Rev. A* **91**, 033830 (2015).
- [63] B. He, S.-B. Yan, J. Wang, and M. Xiao, Quantum noise effects with Kerr-nonlinearity enhancement in coupled gain-loss waveguides, *Phys. Rev. A* **91**, 053832 (2015).
- [64] J. D. Teufel, T. Donner, D. Li, J. W. Harlow, M. S. Allman, K. Cicak, A. J. Sirois, J. D. Whittaker, K. W. Lehnert, and R. W. Simmonds, Sideband cooling of micromechanical motion to the quantum ground state, *Nature (London)* **475**, 359 (2011).
- [65] J. Chan, T. P. M. Alegre, A. H. Safavi-Naeini, J. T. Hill, A. Krause, S. Gröblacher, M. Aspelmeyer, and O.

- Painter, Laser cooling of a nanomechanical oscillator into its quantum ground state, *Nature (London)* **478**, 89 (2011).
- [66] E. Verhagen, S. Deleglise, S. Weis, A. Schliesser, and T. J. Kippenberg, Quantum-coherent coupling of a mechanical oscillator to an optical cavity mode, *Nature (London)* **482**, 63 (2012).
- [67] D. F. Walls and G. J. Milburn, *Quantum Optics* (Springer Verlag, Berlin Heidelberg, 2008).
- [68] J. Laurat, G. Keller, J. A. Oliveira-Huguenin, C. Fabre, T. Coudreau, A. Serafini, G. Adesso, and F. Illuminati, Entanglement of two-mode Gaussian states: Characterization and experimental production and manipulation, *J. Opt. B: Quantum Semiclass. Opt.* **7**, S577 (2005).
- [69] V. D'Auria, S. Fornaro, A. Porzio, S. Solimeno, S. Olivares, and M. G. A. Paris, Full Characterization of Gaussian Bipartite Entangled States by a Single Homodyne Detector, *Phys. Rev. Lett.* **102**, 020502 (2009).
- [70] H. Ogawa, H. Ohdan, K. Miyata, M. Taguchi, K. Makino, H. Yonezawa, J.-I. Yoshikawa, and A. Furusawa, Real-Time Quadrature Measurement of a Single-Photon Wavepacket with Continuous Temporal-Mode-Matching, *Phys. Rev. Lett.* **116**, 233602 (2016).
- [71] K. Zyczkowski, P. Horodecki, A. Sanpera, and M. Lewenstein, Volume of the set of separable states, *Phys. Rev. A* **58**, 883 (1998).
- [72] H.-P. Breuer and F. Petruccione, *The Theory of Open Quantum Systems* (Oxford University Press, Oxford, New York, 2002).
- [73] P. Massignan, A. Lampo, J. Wehr, and M. Lewenstein, Quantum Brownian motion with inhomogeneous damping and diffusion, *Phys. Rev. A* **91**, 033627 (2015).